NUMERICAL PREDICTION OF BEAD FORMATION AND BUILD-UP TOWARD WAAM PROCESS OPTIMIZATION

H. BEN HAMOUDA*, I. O. FELICE**, J. P. OLIVEIRA**,***, J. ANTONISSEN*

**Guaranteed B.V., 9060, Zelzate, Belgium*
***Department of Mechanical and Industrial Engineering, NOVA School of Science and Technology | FCT NOVA, Campus de Caparica, 2829-516 Caparica, Portugal*
**** CENIMAT/I3N, Department of Materials Science, NOVA School of Science and Technology, Universidade NOVA de Lisboa, 2829-516 Caparica, Portugal*

DOI 10.3217/978-3-85125-968-1-04

ABSTRACT

Wire and Arc Additive Manufacturing (WAAM) is a promising solution to produce complex shapes with low buy-to-fly ratio outperforming conventional subtractive manufacturing methods. Generally, this approach relies on robot programs that define the printing path based on a set of pre-defined process parameters. To obtain a net shape WAAM part, the printing path requires controlled bead shape estimation in the preprocessing step. Unlike trial-and-error approach, numerical simulation tries to determine the bead shape by solving coupled physical problems such as fluid dynamics (CFD) and heat transfer. In this work, a numerical tool was deployed to predict single and multiple bead formation given three key process parameters: the wire feed speed, torch travel speed, and voltage. Calculations were performed using ER-90S steel alloy as a printing wire and compared to experimental measurements printed using a MIG/MAG process. As a result, prediction of dimensional features such as the bead height (BH) and width (BW) showed a good agreement with the experiment. Furthermore, the effect of the process parameters was investigated and a parametric study was performed to establish a process guideline that feeds the robot printing strategy.

Keywords: WAAM, MIG/MAG, Bead shape prediction, Process optimization, ER-90S.

INTRODUCTION

WAAM technology is gaining more and more research focus as a promising manufacturing solution characterized by its flexibility to produce large parts with relatively complex shapes as well as its high deposition rates of 1-10 kg/hr [1]. This technology consists of a Directed Energy Deposition (DED) process that applies an electric arc on the base material surface to melt a feeding wire and generate deposition patterns. To perform accurate and reproducible deposition process, robotic tools are generally relied upon where a Computer Aided Manufacturing (CAM) program defines the deposition trajectory and the corresponding process parameters. This pre-processing step needs to be consistently built-up because a slight deviation between the CAM model

and the part-to-print geometry can alter critically the deposition quality [2] and, thus, increases the risk to worsen its structural integrity. Therefore, ensuring the fidelity of the deposition path to the real geometry during deposition is an essential step to demonstrate a successful robotic WAAM program and a reproducible defect-free printed part. This challenge attracts the main attention of several researchers who proposed multiple methods to control geometrical accuracy, (i) thermal field measurement [3, 4], (ii) process control based on passive-vision sensing [5], and (iii) model predictive control (MPC) [6]. Nevertheless, the experimental methods are labour intensive and require higher process cost, apart from the implementation complexity. To overcome these problems, some researchers relied on predictive analyses tools to control the bead shape.

Among predictive models, artificial intelligence and physics-based solutions attracted several researchers. Xue et al. [7], Hu et al. [8] and Karmuhilan et al. [9] presented predictive models based on Artificial Neural Network (ANN) and genetic algorithms to optimize the initial weights and thresholds of the network linking the welding process parameters and the weld shape and, thus, provide more accurate predictions of the bead shape. Their methods, although giving relatively low prediction errors, require significant effort in building up an extended experimental database, which can be quite costly.

Physics-based models consist generally in solving the thermal problem at the contact between the feeding wire and the substrate. Consequently, the bead shape starts forming progressively during the mixing step and its control is controlled by the thermophysical parameters such as the surface tension and the solidification path. The material deposition at the heated zone is tracked via a coupling with a fluid dynamic model [10]. These models showed generally a strength in tracking the thermophysical parameters evolution during the building process and thus, building complete knowledge of the deposition mechanism. However, some improvement in the coupling method is necessary to reduce the computational cost.

In this work, a physical-based model was utilized to simulate the single bead shape formation considering the material's thermophysical properties. The model couples conventional heat transfer equation with fluid compensation model to assess the thermal field and bead shape formation, respectively. Furthermore, a set of experiences were performed within this work to validate the simulation part. Once validated, the effect of the process parameters on the bead geometry was studied.

EXPERIMENTAL PROCEDURE

The ER-90S welding wire was utilized as a deposition wire for the Conventional Gas Metal Arc Welding (GMAW) process (also known as MIG/MAG). A structural ASTM A36 hot-rolled plate with dimensions of 10x80x200 mm^3 was considered as the base plate. The general deposition characteristics are given in Table 1.

Table 1 Deposition process parameters for the ER-90S material

Wire diameter	1 mm
Bead-on-plate length	150 mm
Contact tip to work distance	10 mm
Shielding gas	18% CO_2 + 82% Ar
Shielding gas flow	15 l/min

The experimental procedure to parametrize the welding beads for a Wire and Arc Additive Manufacture (WAAM) process (and then HF-WAAM) and evaluate the weld bead geometry as a function of the wire feed speed (WFS), travel speed (TS), and voltage (U) variables involved the deposition of beads in 15 different combinations, defined by a Box-Behnken Design of Experiments (DOE). As this work aimed to reproduce the geometrical characteristics of the beads, 2 repetitions of the DOE central point were excluded, and then, 13 experiments were analysed and are presented in Table 2. The process used a Pro MIG 3200 power source with a constant voltage dynamic characteristic, which lead to a fixed arc length during deposition, and a Pro MIG 501 control unit. An in-house 3-axis moving table was used to position the plates where the deposition occurred.

Table 2 Description of the plan of experience

	Experiments												
Variables	1	2	3	4	5	6	7	8	9	10	11	12	13
WFS (m/min)	3	7	3	7	3	7	3	7	5	5	5	5	5
TS (mm/min)	240	240	480	480	360	360	360	360	240	240	480	360	480
U (V)	21	21	21	21	18	18	24	24	18	24	24	21	18

After deposition, the beads were cut in three different positions along the weld bead, always neglecting 30 mm of the extremes to avoid possible negative effects regarding the lack of electrical arc stability. They were grinded, polished, and etched with Nital 2% to evaluate the geometrical aspects, under the output average parameters BW (bead width), BH (bead height), CA (contact angle), and P (penetration), shown in

Fig. 1. Figures of the cross-section were obtained using an Olympus CP21 optical microscope and adjusted using the image software Adobe Photoshop C26. The measurements were performed using the license-free software ImageJ. The deposition rate (DR) and arc energy (AE) were also calculated from the measured data of voltage and current, acquired by an Arduino automation system, and mass before and after deposition obtained with a precision scale.

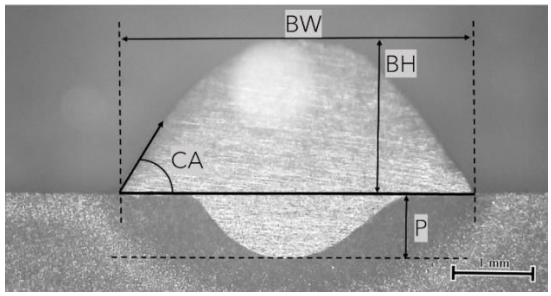

Fig. 1 Bead macrography with a detailed description of geometrical parameters; BH: bead height, BW: bead width, CA: contact angle and P: penetration depth

NUMERICAL PROCEDURE

The physical model presented in this work is implemented in a software developed by ISF Aachen for the numerical simulation of the weld seam shape and the temperature, designed originally for GMAW of steel and aluminium [11]. The model description is similar to that shown in reference [12] where some assumptions were made to propose a good cost-accuracy trade-off. The simplified approach is now 2.5D, instead of a full 3D approach in [12], where the weld pool geometry is solved at the cross-section and the third dimension is computed by linear extrusion along the x direction Fig. 2.

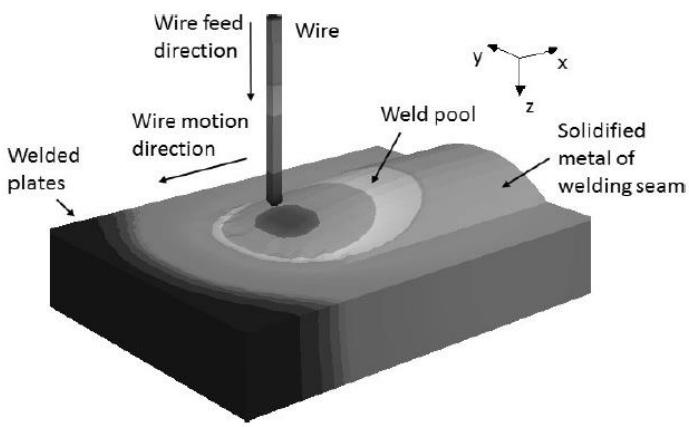

Fig. 2 Schematic presentation of the single bead printing process (GMAW) [12]

Three main sub-models are included in this tool and the corresponding main factors are given in Table 3.

Table 3 Present implemented sub-models and their corresponding parameters

Sub-model	Parameters
Heat source	heat conduction in wire, Ohmic heating, contact resistance, anode, cathode and arc column, electromagnetic force
Heat flow	cathode, drop and arc heat sources, T-dependent material properties, Latent heat of fusion, Influence of non-flat surface
Free surface	Arc pressure distribution, gravitation, mass balance, melting isotherm as boundary condition

The different sub-models are interacting as described in Fig. 3. To speed-up the calculations, a weak coupling was applied between the sub-models enabling less iterations to compute the bead geometry and the heat flow. Consequently, some reverse effects such as the influence of the surface deformation on the processes inside the arc are not considered in this tool.

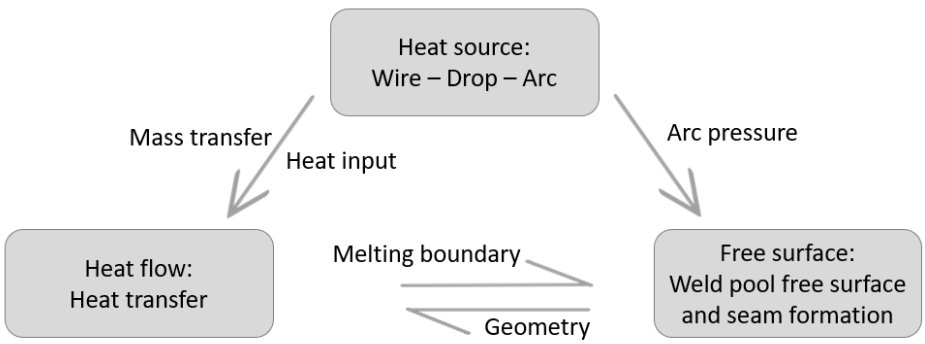

Fig. 3 Sub-models interaction for the simulation of the bead shape formation [11]

The coupling of the sub-models shown in Fig. 3 is done in an iterative way following this procedure:

(i) Calculation of arc heat, wire melting, droplets heat and mass
(ii) Calculation of heat source distribution
(iii) Calculation of mass source distribution
(iv) Calculation of heat transfer
(v) Extraction of liquid area
(vi) Calculation of weld pool surface deformation
(vii) Mesh transformation

Within the same iteration, the average weld pool is assessed by solving the arc-droplet-wire part model (i) in the transient where the heat transfer ((ii)..(iv)) and the weld seam ((v)..(vii)) sub-models are solved in a quasi-steady-state.

The heat transfer is assessed via heat conservation equations given for (1) conductive and (2) convective transfers. The two equations are solved using the discrete differences and discrete volume methods, respectively. The sum of the two solutions at the same time

gives the effect of the two process concurrently. The effects of electro-magnetic force, gravitation and surfaces forces are included in the discrete volume equivalent of the momentum conservation algorithm that is defined together with a continuum conservation algorithm to capture the changing in the discrete volume positions.

$$\frac{\partial(\rho h)}{\partial t} = \text{div}(\lambda\, grad T) + Q \quad (1)$$

$$\frac{\partial(\rho h)}{\partial t} = \text{div}(h\rho\vec{u}) \quad (2)$$

In Eqn. (1) and (2), h denotes the enthalpy, T: temperature; ρ: density; Q: arc heat input; λ: thermal conductivity; $\vec{u}$: velocity of the convective heat transfer.

The weld pool/seam is computed by solving the Computational Fluid Dynamics (CFD) problem in a quasi-steady state regime using the Lattice-Boltzman approach [13]. The fluid flow compensation method is used for this purpose to compute the droplet mass and velocity at the contact with the arc weld seam considering these effects:

- The flow from cathode area (Fig. 4-(a));
- The effect of the droplet moving in the droplet effect area (Fig. 4-(b));
- The effect of surface forces in the back area of the weld pool.

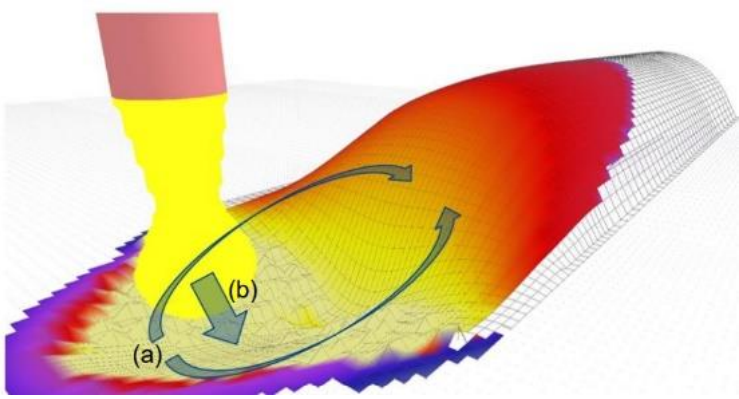

Fig. 4 Fluid flows in the weld pool derived from (a) cathode areas and (b) droplet impulse

RESULTS AND DISCUSSION

The bead morphological parameters summarized in Fig. 1 are important input parameters to use in the CAM program. For instance, the bead height (BH) represents the first layer height to be considered in the part slicing step whereas the bead width (BW) parameter is used to define the best overlapping to be applied for an optimal layer build-up [14].

SINGLE BEAD SIMULATION

It is important at this step to notice that the model translates the input process parameters into an equivalent heat source equation known as the double ellipsoid Goldak equation [15]. The shape, given in Fig. 5-(a), shows the seam front and gear ellipsoidal forms that are representing the heat distribution during the building process. An example of the obtained temperature map is given in Fig. 5-(b) confirming the approximation of the double-ellipsoidal heat shape. The different parameters of the Goldak equations are predicted and presented in the appendix (Table 4).

(a)

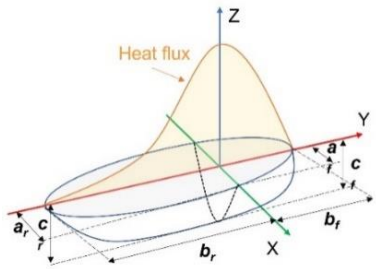

(b)

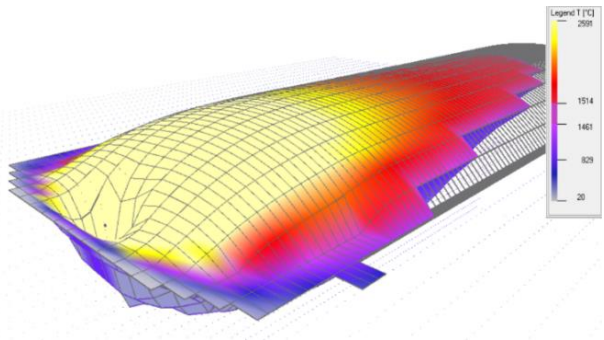

Fig. 5 (a) double ellipsoid Goldak equation (b) Temperature distribution during the weld seam formation

The obtained results are given in Fig. 6 for three parameters: the bead height (BH), the bead width (BH) and the contact angle (CA). For the bead height, the obtained values are ranging between 1.7mm and 4.1mm depending on the input process parameters which are controlling the heat input. Compared to the experimental measurements, the result showed acceptable prediction errors (average ~17%). For the bead width, results show values varying from 2 to 11 mm. Compared to the experimental results, a higher prediction error was obtained (average ~ 29%). Finally, the contact angle values are comparable to the experimental values within an error range of 21%. The deviations from the experimental results can be explained by the assumptions that were applied to the mathematical model and are more pronounced on the BW and CA parameters. In this

scope, the analyses of the effect of each process parameter on BH and BW mainly could help to explain the origin of these deviations. This task is made in the following section.

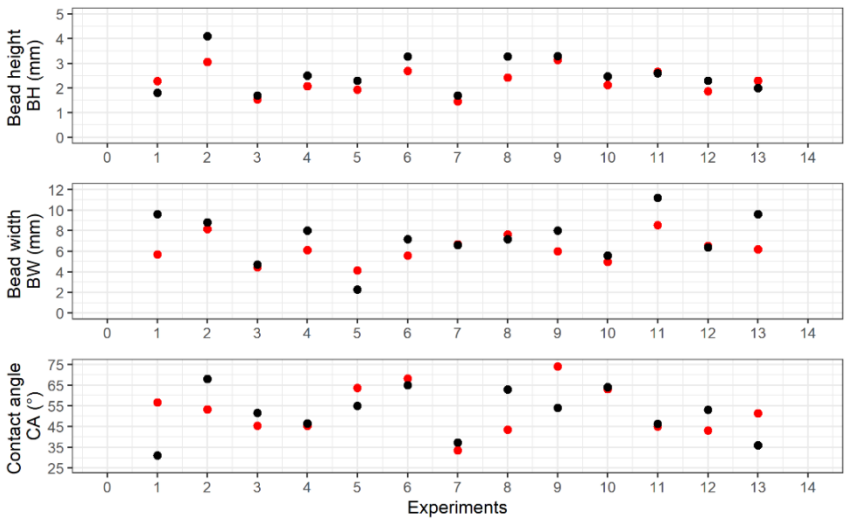

Fig. 6 Comparison of the predicted (black dots) and experimental (red dots) bead shape parameters

The predicted thermal cycles corresponding to the different experiments are shown in Fig. 7. These profiles were extracted at the centre of the bead for each experiment. Nevertheless, there was no experimental measurement provided to validate this result, work on progress.

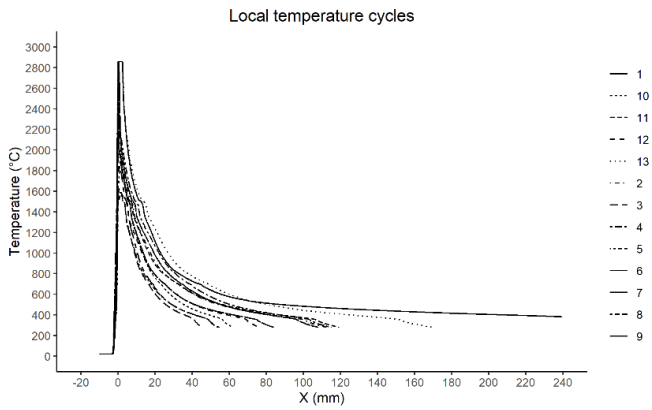

Fig. 7 Local temperature profiles at the centre of the bead for all the experiments

EFFECT OF THE PROCESS PARAMETERS

The results introduced above consist of a validation step that will be followed by a sensitivity analysis of process parameters (TS, WFS and U) to inspect their influence on the bead shape parameters. Results are given in Fig. 8. These results show a clear non-proportional effect of the torch travel speed versus the bead height and width. This can be explained by the fact that increasing the TS decreases drastically the arc heat input leading to a smaller bead shape. For the other parameters, there is no clear effect on the bead geometry.

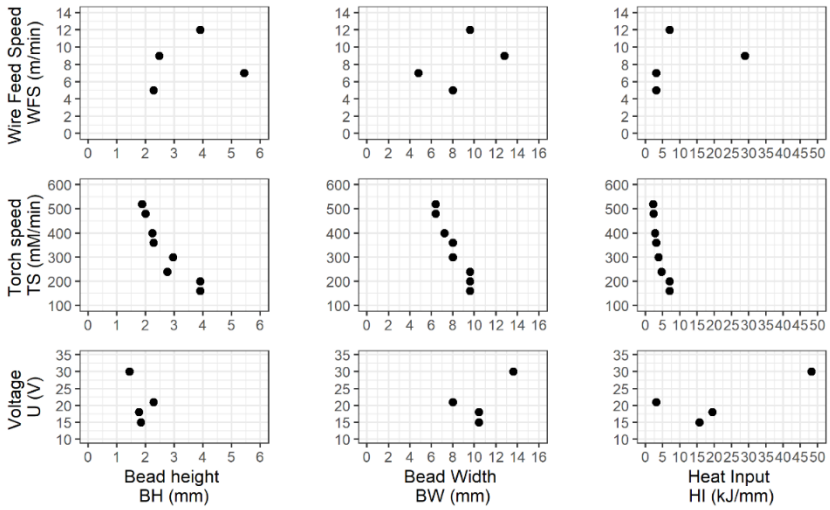

Fig. 8 Effect of WFS, TS and U parameters on BH, BW and HI of the ER-90S material

CONCLUSIONS

Physical modelling helps not only by making fast predictions of the bead geometrical parameters but also by tracking the interaction between the different phenomena coexisting during the printing. In this paper, the focus is made on the bead geometry because of its importance as an input to the robotic WAAM program. The simulated bead height represents the layer thickness whereas the bead width is crucial to define the best overlapping inter-beads. The simulation results for the bead height showed acceptable results in the range of ±20% compared to the experimental measurements. Furthermore, the parametric study showed the importance of the torch travel speed to control the bead shape via the control of its heat input. Similar investigations of other materials can generate a helpful guideline to control the bead shape and, thus, the printing process with higher quality.

MATHEMATICAL SYMBOLS AND UNITS

WFS: wire feed speed (m/min)
TS: travel speed (mm/min)
U: voltage (V)
BW: bead width (mm)
BH: bead height (mm)
CA: contact angle (°)
P: penetration (mm)
DR: deposition rate
AE: arc energy AE (kJ/mm)
T: Temperature (°C)
h: enthalpy (J/m^3)
ρ: density (kg/m^3)
Q: arc heat input (J/mm)
λ: thermal conductivity (W/(m·K))
$\vec{u}$: velocity of the convective heat transfer

APPENDICES

Table 4 Predicted parameters of the Goldak equation

Experience	1	2	3	4	5	6	7	8
Qf(W)	3983	2579.7	998.65	2245.1	1313	2673.2	849.49	2673.2
Qr(W)	2235.9	998.57	646.94	2412.8	520.44	1657.2	874.11	1657.2
af(mm)	0.8	0.8	0.4	0	0	0.4	0	0.4
ar(mm)	15.2	13.2	6.4	14.8	6.4	14	7.6	14
bf(mm)	4.8	3.6	2.36	3.2	2.4	3.2	2.83	3.2
cf(mm)	5.59	1.44	0.32	1.37	0.48	1.36	0.77	1.36
Q(W)	6218.9	3578.3	1645.6	4657.9	1833.5	4330.4	1723.6	4330.4
ff	1.28	1.44	1.21	0.96	1.43	1.23	0.99	1.23
fr	0.72	0.56	0.79	1.04	0.57	0.77	1.01	0.77
br(mm)	4.8	3.6	2.36	3.2	2.4	3.2	2.83	3.2
cr(mm)	5.59	1.44	0.32	1.37	0.48	1.36	0.77	1.36

Experience	9	10	11	12	13
Qf(W)	2143.1	1782.4	1636.5	1615.2	6047.1
Qr(W)	777.62	1064.3	1130.4	1134.8	1851.3
af(mm)	0.8	0	0.4	0	1.2
ar(mm)	9.2	9.6	11.2	8.8	17.6
bf(mm)	3.6	2	5.6	3.2	4.8
cf(mm)	1.27	0.82	1.3	0.52	2.42
Q(W)	2920.7	2846.6	2766.8	2749.9	7898.4
ff	1.47	1.25	1.18	1.17	1.53
fr	0.53	0.75	0.82	0.83	0.47
br(mm)	3.6	2	5.6	3.2	4.8
cr(mm)	1.27	0.82	1.3	0.52	2.42

ACKNOWLEDGEMENTS

This activity has received funding from the European Institute of Innovation and Technology (EIT) – Project Smart WAAM: Microstructural Engineering and Integrated Non-Destructive Testing. This body of the European Union receives support from the European Union's Horizon 2020 research and innovation program. IOF and JPO acknowledge the Portuguese Fundação para a Ciência e a Tecnologia (FCT - MCTES) for its financial support via the project UID/EMS/00667/2019 (UNIDEMI). JPO acknowledges the funding of CENIMAT/i3N by national funds through the FCT-Fundação para a Ciência e a Tecnologia, I.P., within the scope of Multiannual Financing of R&D Units, reference UIDB/50025/2020-2023.

References

[1] C. R. CUNNINGHAM, J. M. FLYNN, A. SHOKRANI, V. DHOKIA, S. T. NEWMAN: 'Strategies and processes for high quality wire arc additive manufacturing', Invited review article in *Additive Manufacturing*, 22, 672-686, 2018, https://doi.org/10.1016/j.addma.2018.06.020.

[2] Y. LI, Q. HAN, G. ZHANG, I. HORVÁTH: 'A layers-overlapping strategy for robotic wire and arc additive manufacturing of multi-layer multi-bead components with homogeneous layers', *The International Journal of Advanced Manufacturing Technology*, 96, 3331-3344, 2018, https://doi.org/10.1007/s00170-018-1786-3.

[3] V. L. JORGE, F. R. TEIXEIRA, A. SCOTTI: 'Pyrometrical Interlayer Temperature Measurement in WAAM of Thin Wall: Strategies, Limitations and Functionality', *Metals*, 12, 2022, https://doi.org/10.3390/met12050765.

[4] J. XIONG, Y. ZHANG, Y. PI: 'Control of deposition height in WAAM using visual inspection of previous and current layers', *Journal of Intelligent Manufacturing*, 32, 2209-2217, 2021, https://doi.org/10.1007/s10845-020-01634-6.

[5] Y. HUANG, S. HOU, L. YANG, G. TIAN, Z. YONG, S. LIU: 'Effect of arc dynamic behavior on deposition quality of additive manufactured aluminum alloys', *Journal of Materials Processing Technology*, 295, 117172, 2021, https://doi.org/10.1016/j.jmatprotec.2021.117172.

[6] C. XIA, Z. PAN, S. ZHANG, J. POLDEN, L. WANG, H. LI, Y. XU, S. CHEN: 'Model predictive control of layer width in wire arc additive manufacturing', *Journal of Manufacturing Processes*, 58, 179-186, 2020, https://doi.org/10.1016/j.jmapro.2020.07.060.

[7] Q. XUE, S. MA, Y. LIANG, J. WANG, Y. WANG, F. HE, M. LIU: 'Weld Bead Geometry Prediction of Additive Manufacturing Based on Neural Network', *11th International Symposium on Computational Intelligence and Design (ISCID)*, pp. 47-51, 2018 https://doi.org/10.1109/ISCID.2018.10112.

[8] Z. HU, X. QIN, Y. LI, N. MAO: 'Welding parameters prediction for arbitrary layer height in robotic wire and arc additive manufacturing', *Journal of Mechanical Science and Technology*, 34, 1683-1695, 2020, https://doi.org/10.1007/s12206-020-0331-0.

[9] M. KARMUHILAN, A. KUMAR SOOD: 'Intelligent process model for bead geometry prediction in WAAM', *Materials Today*, Proceedings 5, 24005-24013, 2018, https://doi.org/10.1016/j.matpr.2018.10.193.

[10] X. BAI, P. COLEGROVE, J. DING, X. ZHOU, C. DIAO, P. BRIDGEMAN, J. R. HÖNNIGE, H. ZHANG, S. WILLIAMS: 'Numerical analysis of heat transfer and fluid flow in multilayer deposition of PAW-based wire and arc additive manufacturing', *International Journal of Heat and Mass Transfer*, 124, 504-516, 2018, https://doi.org/10.1016/j.ijheatmasstransfer.2018.03.085.

[11] T. LOOSE, O. MOKROV, U. REISGEN: '"SimWeld" and "DynaWeld" - Software tools to set up simulation models for the analysis of welded structures with "LS-Dyna"', *Welding and cutting*, 15, 168-172, 2016.

[12] O. MOKROV, O. LYSNYI, M. SIMON, U. REISGEN, G. LASCHET, M. APEL: 'Numerical investigation of droplet impact on the welding pool in gas metal arc welding', *Materialwissenschaft und Werkstofftechnik*, 48, 1206-1212, 2017, https://doi.org/10.1002/mawe.201700147.

[13] S. CHEN and G. D. DOOLEN: 'Lattice Boltzmann Method for Fluid Flows', *Annu. Rev. Fluid Mech.*, 30:329-364, 1998.

[14] Y. LI, Q. HAN, G. ZHANG, I. HORVÁTH: 'A layers-overlapping strategy for robotic wire and arc additive manufacturing of multi-layer multi-bead components with homogeneous layers', *The International Journal of Advanced Manufacturing Technology*, 96, 3331-3344, 2018, https://doi.org/10.1007/s00170-018-1786-3.

[15] J. A. GOLDAK, A. P. CHAKRAVARTI, M. BIBBY: 'A new finite element model for welding heat sources', *Metallurgical Transactions B*, 15, 299-305, 1984.